PROCEEDINGS OF SCIENCE

GeV gamma-ray detection from intense GRB 240529A during the afterglow's shallow decay phase

Kenta Terauchi,* **Katsuaki Asano and Tomohiko Oka**

Department of Physics, Kyoto University,
Kitashirakawa Oiwake-cho, Sakyo, Kyoto, 606-8502, Japan
Institute for Cosmic Ray Research, the University of Tokyo,
5-1-5 Kashiwanoha, Kashiwa, Chiba 277-8582, Japan
Research Organization of Science and Technology, Ritsumeikan University,
1-1-1 NojiHigashi, Kusatsu, 525-8577, Shiga, Japan

E-mail: terauchi.kenta.74s@st.kyoto-u.ac.jp

X-ray light curves of gamma-ray burst (GRB) afterglows exhibit various features, with the shallow decay phase being particularly puzzling. While some studies report absence of the X-ray shallow decay for hyper-energetic GRBs, recently discovered GRB 240529A shows a clear shallow decay phase with an isotropic gamma-ray energy of 2.2×10^{54} erg, making it a highly unusual case compared to typical GRBs. In order to investigate the physical mechanism of the shallow decay, we perform the *Fermi*-LAT analysis of GRB 240529A along with *Swift*-XRT analysis. We find no jet break feature in the X-ray light curve and then give the lower bound of the collimation-corrected jet energy of $> 10^{52}$ erg, which is close to the maximum rotational energy of a magnetar. Our LAT data analysis reveals GeV emission with a statistical significance of 4.5σ during the shallow decay phase, which is the first time for hyper-energetic GRBs with a typical shallow decay phase. The GeV to keV flux ratio is calculated to be 4.2 ± 2.3. Together with X-ray spectral index, this indicates an inverse Compton origin of the GeV emission. Multiwavelength modeling based on time-dependent simulations tested two promising models, the energy injection and wind models. While the energy injection model shows a tension with LAT data, both models can explain the X-ray and GeV data. We present our results along with the future prospects of the current or next generation gamma-ray telescopes for distinguishing between the shallow decay models. For full details of the results, see the published paper [1].

39th International Cosmic Ray Conference (ICRC2025)
15–24 July 2025
Geneva, Switzerland

ICRC 2025
The Astroparticle Physics Conference
Geneva July 15-24, 2025

*Speaker

PoS(ICRC2025)862

1. Introduction

X-ray afterglows in a large fraction of GRBs (approximately 90%; see [2, 3]) show a shallow decay behavior ($f_\nu \propto T^{-0.5}$ or shallower) during initieal $\sim 10^3$ s [4, 5]. Although the origin of the shallow decay is still largely unknown, it is generally believed to be related to the central engine of GRBs. Several models are proposed to explain the shallow decay such as the energy injection model [6–8], evolving microphysical parameters [9–11], and the wind model [12, 13]. While a long activity of the central engine, such as a magnetar, has been considered for the energy injection model [7], [14] show that the finite thickness of the ejecta can naturally cause the evolution of the forward shock equivalent to the energy injection model. The wind model is also attractive. Unlike the energy injection model, it does not require a long activity for the central engine with a non-trivial evolution of the luminosity or bulk Lorentz factor [12, 13]. As shown in [15], GeV–TeV gamma-ray observations can provide clues to understand the shallow decay phase.

The detection of GRB 240529A was initially reported by the Burst Alert Telescope (BAT; [16]) on the *Neil Gehrels Swift Observatory* (*Swift*) spacecraft on 29 May 2024, 02:58:31 UT (hereafter T_0; [17]). The prompt duration T_{90} (the time corresponding to 5%–95% of a burst fluence) is 160.67 ± 14.52 s in the 15–350 keV band. There was no onboard trigger of the prompt emission by the *Fermi* Gamma-Ray Burst Monitor. The X-Ray Telescope (XRT; [18]) on *Swift* started observations of GRB 240529A 107 s after BAT trigger [19]. From its X-ray light curve, the afterglow shows shallow decay expressed by a temporal index of -0.21 ± 0.03, followed by a steeper decay than usual cases with a temporal index of -2.02 ± 0.04 with a break at $1.63(5) \times 10^4$ s. 0.3–10 keV energy flux during the shallow decay phase is approximately 2×10^{-10} erg cm^{-2} s^{-1}, which is one of the brightest shallow decay in X-rays [20–22].

Given the fluence measurement of $S_\gamma = 1.3^{+0.4}_{-0.5} \times 10^{-4}$ erg cm^{-2} (20 keV − 10 MeV) by Konus-*Wind* and the redshift measurement of $z = 2.695$ by GTC telescope [23], the isotropic-equivalent gamma-ray energy of the prompt emission, $E_{\gamma,\mathrm{iso}}$ is estimated to be $E_{\gamma,\mathrm{iso}} = 2.2^{+0.7}_{-0.8} \times 10^{54}$ erg [24], which makes the GRB an energetic event among GRB population. GRB 240529A possess the most shallow decay index of 0.2 among hyperenergetic GRBs with $E_{\mathrm{iso}} > 10^{54}$ erg, while other bursts show steeper decay index than the typical value of 0.5, making GRB 240529A a unique event with an evident X-ray shallow decay feature. Due to its characteristics, GRB 240529A may offer insights into the physical mechanism behind the shallow decay phase.

In this work, we present the *Fermi*-LAT analysis of GRB 240529A and the multi-wavelength modeling, together with the future prospect. The details of the analysis and the results are described in [1].

2. *Fermi*-LAT Analysis

We use 6×10^5 s of data of Pass 8 SOURCE class data [25, 26] between 100 MeV and 10 GeV. The upper bound of the energy is chosen to be 10 GeV, since an absorption by extragalactic background light (EBL) starts to be non-negligible in the higher energies. Events within 20° of the GRB position (enhanced XRT position: R.A., decl. = 335.°358, +51.°562) are extracted. Events detected at zenith angles larger than 100° were excluded to limit the contamination from gamma rays generated by cosmic ray interactions in the upper layers of Earth's atmosphere.

We performed an unbinned likelihood analysis with the latest Fermitools package (v2.2.0), utilizing the `P8R3_SOURCE_V3` instrument response function. The region of interest (ROI) is modeled from the latest *Fermi*-LAT source catalog based on 14 yr of data, 4FGL (data release 4, [27]) for point and extended sources that are within 15° of the ROI center, as well as the latest Galactic diffuse and isotropic diffuse templates (`gll_iem_v07.fits` and `iso_P8R3_SOURCE_V3_v1.txt`, respectively). Throughout the analysis, the spectral parameters of the 4FGL sources were kept fixed to the values from the catalog.

The background components were first determined using the data up to 6×10^5 s since T_0. The obtained best-fit spectral parameters of the background components were fixed and used for the further analysis. Then, we computed count and test statistic (TS) maps in order to search for any residual gamma-ray emission. The TS value is defined to be the natural logarithm of the ratio of the likelihood of one hypothesis (e.g., presence of one additional source) and the likelihood for the null hypothesis (e.g., absence of source). Note that there were no gamma-ray events between T_0 and $t = 1 \times 10^3$ s due to the ROI outside of LAT's field of view, and hence the maps were generated with time intervals after $t = 1 \times 10^3$ s. The first time interval (1×10^3 s–5×10^4 s) is chosen to cover the X-ray shallow decay phase with a sufficient margin of time. From the TS maps, we discovered a point-like gamma-ray source coincident in position with GRB 240529A in the time range of 1×10^3 s–5×10^4 s. This is the first GeV discovery for the shallow decay GRBs with $E_{\rm iso} > 10^{54}$ erg with a typical shallow decay. No significant source is found at times beyond $t = 5 \times 10^4$ s.

We localized the point source with `gtfindsrc` to find the best-fit position and uncertainty. The localized position for the new gamma-ray source is offset by $0.^\circ 05$ from the exact position of GRB 240529A (R.A., decl. = $335.^\circ 358$, $+51.^\circ 562$) and has R.A., decl. = $335.^\circ 43$, $+51.^\circ 59$ (J2000). The corresponding 95% positional uncertainty radius is $r = 0.^\circ 18$, indicating a good consistency between the GRB position and the localized position.

To model the gamma-ray emission coincident with GRB 240529A, we added a point source at the GRB position to the source model. We set the spectrum to `PowerLaw2` model, with its photon index fixed to 2.0 or allowed to vary. The returned TS value for the case of the fixed photon index is 20, corresponding to a detection significance of 4.5σ.

3. Modeling and Discussion

From *Fermi*-LAT spectral analysis, the flux ratio between the GeV and keV energy ranges is $F_{\rm GeV}/F_{\rm keV} = 4.2 \pm 2.3$, strongly suggesting that the GeV emission arises from an inverse Compton component rather than a synchrotron component. This is also supported by the photon index of 2.1 obtained from the XRT spectrum, which is difficult to explain the obtained LAT flux by the extrapolation of the XRT spectrum. To produce an efficient inverse Compton emission, a high Compton parameter Y is necessary, indicating a low energy fraction of the magnetic field ϵ_B, or high energy fraction of electrons $\epsilon_{\rm e}$ and large blastwave energy $E_{\rm K,iso}$.

To reproduce the lightcurves and spectra, primarily focusing on the behavior during the shallow decay phase, we adopt the simulation code in [15], in which the shallow decay afterglow is discussed with time-dependent simulations. The code was developed in [28] [see also, 29]. The evolution of the electron and photon energy distributions in the shocked region is followed taking into account particle injection, synchrotron emission, synchrotron self-absorption, inverse Compton (IC)

emission, $\gamma\gamma$-absorption, electron–positron pair creation, adiabatic cooling, and photon escape. The bulk Lorentz factor Γ of the shocked region is self-consistently solved with the energy conservation law. The photon flux for observers is calculated considering the Doppler beaming and the surface curvature.

Here we adopt two models for the shallow decay phase: the energy injection model [6–8] and the wind model [12, 13]. Both models reproduce the X-ray flux and spectrum during the shallow decay phase ($T - T_0$: $600 - 1.6 \times 10^4$ s), with the X-ray flux consistent within a factor of 2. Concerning the GeV light curve during the shallow decay phase, we compared the mean model flux, calculated between $(T_0+)1\times10^3 - 1.6\times10^4$ s, with the LAT data. Both models yielded no significant differences with respect to the LAT data, showing less than 1σ deviations. In reproducing the GeV flux, the large ϵ_e and small ϵ_B in the energy injection model are required to realize the observed GeV flux by synchrotron self-Compton (SSC) emission and the X-ray flux ($\propto \epsilon_e^{p-1}\epsilon_B^{(p+1)/4}$) by synchrotron emission keeping the synchrotron peak frequency $\nu_m \propto \epsilon_e^2\epsilon_B^{1/2}$ high enough to suppress the optical flux. In the energy injection model, the electron minimum Lorentz factor γ_m is much higher than that for the wind model. Therefore, the spectral peak frequency (~ 0.1 TeV) of the SSC component is much higher than that of the wind model (~ 1 GeV). Therefore, the intrinsic TeV flux is suppressed in the wind model compared to the energy injection model. Both models require $E_{K,iso}$ exceeding 10^{55} erg, which implies a significant amount of the blastwave kinetic energy, surpassing the radiation energy released during the prompt phase (2.2×10^{54} erg). As for GeV spectrum, the hard spectral index (~ 1.24) in the LAT energy range for the energy injection model is deviated from the LAT result (2.99 ± 0.64) by 2.7σ, while for the wind model case (index ~ 1.91) the deviation is 1.7σ. Thus, the LAT data shows a tension with the energy injection model; however, the limited photon statistics of the LAT data prevent a definitive conclusion. It should be noted that it is easier to reproduce the soft GeV spectrum in the wind model due to its low spectral peak frequency of the SSC component.

4. Future Prospect

In this section, the detectability of shallow decay GRBs with future Cherenkov Telescope Array Observatory (CTAO) is discussed. Here, the modeled time-dependent spectra of GRB 240529A for both the energy injection and the wind model are used for the target of this study. As demonstrated in [15], a precise measurement of the GeV light curve and the spectral evolution during the shallow decay phase is crucial to identify the physical mechanism behind the shallow decay.

In order to study whether the future CTAO is capable of detecting the temporal evolution of the spectrum, differential sensitivity for different integration times are simulated. The calculation of the sensitivity is performed using `gammapy`, adopting the official instrument response functions of four LSTs [30]. The wobble offset is assumed to be 0.6°, which is larger than the standard value used for point source observations of LST-1. This value is chosen to take into account the worse PSF in low energies near threshold, thus the sufficient number of background region can be applied. Note that the offset value needs to be optimized once the PSF for full LST array is evaluated. The event selection cuts are already applied to the IRFs based on the observation time (1800 s and 18000 s). Zenith angle is selected to be 20° to test the best performance of LSTs in low energies.

The observation is defined as follows. The observation is divided into five consecutive blocks starting from 500 s until 10^5 s, which are logarithmically spaced in time. A time duration of observation is computed for each block, which is simply a total time length of each block. Taking into account the real observation, the maximum observation time per block is set to 4 hours. A reference time is defined to be a geometric mean of each block, and the spectrum at each reference time resembles the spectrum during each block.

The calculated 5σ differential sensitivity for each observation block is presented in Figure 1 along with the reproduced spectra of GRB 240529A for the both models. As for the energy injection model one can see that VHE emission can be well detected for all observation blocks, while for the wind model VHE emission can be well detected in 4200–35000 s (1.2–9.6 h) and barely detected in 1400–4200 s (0.4–1.2 h). Given that both models are detectable few thousand seconds after the GRB trigger, the fast reaction to the GRB trigger is not quite necessary to study VHE emission of GRBs with shallow decay phase.

It should be noted that GRB 240529A-like event can be detected even under a strong EBL attenuation for a redshift $z = 2.7$. This redshift value is significantly greater than the highest redshift of $z = 1.1$ ever detected by ground-based TeV instruments [31], demonstrating the detection power of future LST array.

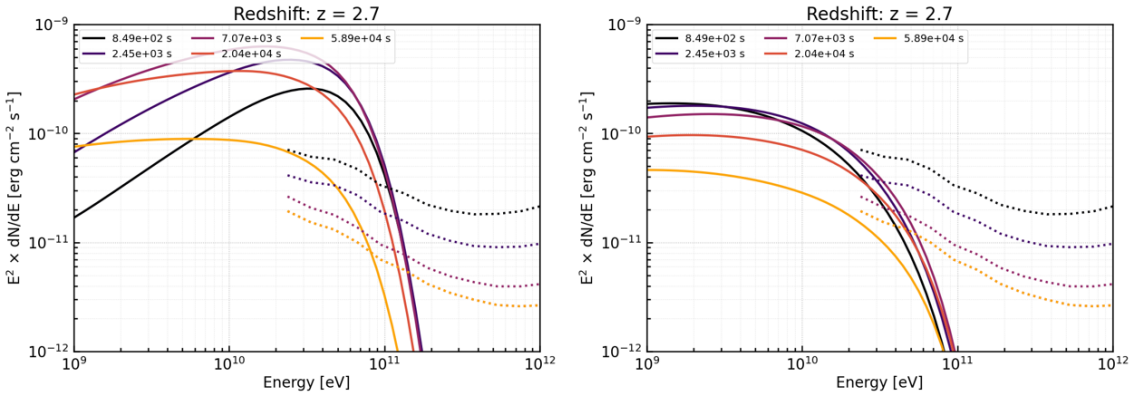

Figure 1: Time-resolved differential sensitivity (dotted line) of future LST arrays plotted along time-resolved spectra (solid line) of GRB 240529A predicted by energy injection (left) and wind (right) model. Colors correspond to reference times of observation blocks (see text). Note that maximum observation time per block is set to be 4 hours, thus there are only 4 curves for the sensitivity (the yellow dotted line represents the sensitivity for the last two observation blocks).

5. Summary

Recently discovered GRB 240529A has an extremely large isotropic gamma-ray energy release of 2.2×10^{54} erg and a prominent X-ray shallow decay phase with a decay index of 0.2, indicating that the burst is a unique case which provides a valuable key to understanding the physical process of the shallow decay phase. In this work, we presented *Fermi*-LAT analysis of GRB 240529A, indicating the evidence of GeV emission (4.5σ) covering the X-ray shallow decay phase of the GRB. The flux level of the GeV emission is 4.2 ± 2.3 times larger than the keV flux, suggesting that the

GeV emission is dominated by strong IC emission. We performed the multiwavelength modeling based on the time-dependent simulations and tested the two promising models of the shallow decay phase: the energy injection model and the wind model. Both models reproduce the X-ray and GeV data during the shallow decay phase, though the GeV spectrum indicates some tension with the energy injection model. Although distinguishing between them requires better statistics, our modeling shows that gamma-ray observations are a useful tool in constraining the shallow decay models. Future GeV–TeV observations by CTAO will play a pivotal role in constraining models of the shallow decay phase as demonstrated in this work.

Acknowledgments

This research has made use of Fermi data obtained through High Energy Astrophysics Science Archive Research Center Online Service, provided by the NASA/Goddard Space Flight Center. This work made use of data supplied by the UK Swift Science Data Centre at the University of Leicester. This research has made use of the CTA instrument response functions provided by the CTA Consortium and Observatory, see https://www.cta-observatory.org/science/cta-performance/ (version prod5 v0.1; [30]) for more details. This work is supported by a Grant-in-Aid for JSPS Fellows Grant Nos. 23KJ1222 (KT) and 23KJ2094 (TO), and KAKENHI grant Nos. 22K03684, 23H04899, and 24H00025 (KA). This research was supported by a grant from the Hayakawa Satio Fund awarded by the Astronomical Society of Japan.

References

[1] K. Terauchi, T. Oka and K. Asano, *Evidence for gev gamma-ray emission from intense grb 240529a during the afterglow's shallow decay phase*, *The Astrophysical Journal* **986** (2025) 189.

[2] R. Yamazaki, Y. Sato, T. Sakamoto and M. Serino, *Less noticeable shallow decay phase in early X-ray afterglows of GeV/TeV-detected gamma-ray bursts*, *Monthly Notices of the Royal Astronomical Society* **494** (2020) 5259 [https://academic.oup.com/mnras/article-pdf/494/4/5259/33192737/staa1095.pdf].

[3] E.-W. Liang, H.-J. Lü, S.-J. Hou, B.-B. Zhang and B. Zhang, *A comprehensive analysis of swift/x-ray telescope data. iv. single power-law decaying light curves versus canonical light curves and implications for a unified origin of x-rays*, *The Astrophysical Journal* **707** (2009) 328.

[4] J.A. Nousek, C. Kouveliotou, D. Grupe, K.L. Page, J. Granot, E. Ramirez-Ruiz et al., *Evidence for a canonical gamma-ray burst afterglow light curve in the swift xrt data*, *The Astrophysical Journal* **642** (2006) 389.

[5] E.-W. Liang, B.-B. Zhang and B. Zhang, *A comprehensive analysis of swift xrt data. ii. diverse physical origins of the shallow decay segment*, *The Astrophysical Journal* **670** (2007) 565.

[6] B. Zhang and P. Mészáros, *Gamma-ray burst afterglow with continuous energy injection: Signature of a highly magnetized millisecond pulsar*, *The Astrophysical Journal* **552** (2001) L35.

[7] B. Zhang, Y.Z. Fan, J. Dyks, S. Kobayashi, P. Mészáros, D.N. Burrows et al., *Physical Processes Shaping Gamma-Ray Burst X-Ray Afterglow Light Curves: Theoretical Implications from the Swift X-Ray Telescope Observations*, **642** (2006) 354 [astro-ph/0508321].

[8] J. Granot and P. Kumar, *Distribution of gamma-ray burst ejecta energy with Lorentz factor*, *Monthly Notices of the Royal Astronomical Society: Letters* **366** (2006) L13 [https://academic.oup.com/mnrasl/article-pdf/366/1/L13/56929765/mnrasl_366_1_l13.pdf].

[9] Y. Fan and T. Piran, *Gamma-ray burst efficiency and possible physical processes shaping the early afterglow*, *Monthly Notices of the Royal Astronomical Society* **369** (2006) 197 [https://academic.oup.com/mnras/article-pdf/369/1/197/18666631/mnras0369-0197.pdf].

[10] A. Panaitescu, P. Mészáros, D. Burrows, J. Nousek, N. Gehrels, P. O'Brien et al., *Evidence for chromatic X-ray light-curve breaks in Swift gamma-ray burst afterglows and their theoretical implications*, *Monthly Notices of the Royal Astronomical Society* **369** (2006) 2059 [https://academic.oup.com/mnras/article-pdf/369/4/2059/3833121/mnras0369-2059.pdf].

[11] Ioka, K., Toma, K., Yamazaki, R. and Nakamura, T., *Efficiency crisis of swift gamma-ray bursts with shallow x-ray afterglows: prior activity or time-dependent microphysics?*, *A&A* **458** (2006) 7.

[12] R. Shen and C.D. Matzner, *Coasting external shock in wind medium: An origin for the x-ray plateau decay component in swift gamma-ray burst afterglows*, *The Astrophysical Journal* **744** (2011) 36.

[13] H. Dereli-Bégué, A. Pe'er, F. Ryde, S.R. Oates, B. Zhang and M.G. Dainotti, *A wind environment and Lorentz factors of tens explain gamma-ray bursts X-ray plateau*, *Nature Communications* **13** (2022) 5611 [2207.11066].

[14] Y. Kusafuka and K. Asano, *Ejecta Width and Magnetization Reflected in Gamma-Ray Burst Early Afterglows: Implication for Reverse Shock Component and Shallow Decay Phase*, *arXiv e-prints* (2024) arXiv:2408.10750 [2408.10750].

[15] K. Asano, *Multiwavelength Modeling for the Shallow Decay Phase of Gamma-Ray Burst Afterglows*, **970** (2024) 141.

[16] S.D. Barthelmy, L.M. Barbier, J.R. Cummings, E.E. Fenimore, N. Gehrels, D. Hullinger et al., *The burst alert telescope (bat) on the swift midex mission*, *Space Science Reviews* **120** (2005) 143.

[17] R.A.J. Eyles-Ferris, R. Gupta, A.Y. Lien, K.L. Page, D.M. Palmer, T.M. Parsotan et al., *GRB 240529A: Swift detection of a burst with an optical counterpart*, *GRB Coordinates Network* **36556** (2024) 1.

[18] D.N. Burrows, J.E. Hill, J.A. Nousek, J.A. Kennea, A. Wells, J.P. Osborne et al., *The swift x-ray telescope*, *Space Science Reviews* **120** (2005) 165.

[19] S. Dichiara, J.A. Kennea, K.L. Page, A.P. Beardmore, A. Melandri, T. Sbarrato et al., *GRB 240529A: Swift-XRT refined Analysis*, *GRB Coordinates Network* **36564** (2024) 1.

[20] X.-K. Ding, Y.-R. Shi, S.-Y. Zhu, W.-P. Sun and F.-W. Zhang, *Statistical properties of the X-ray afterglow shallow decay phase and their relationships with the prompt gamma-ray emission of gamma-ray bursts*, **367** (2022) 58.

[21] L. Zhao, B. Zhang, H. Gao, L. Lan, H. Lü and B. Zhang, *The shallow decay segment of grb x-ray afterglow revisited*, *The Astrophysical Journal* **883** (2019) 97.

[22] C.-H. Tang, Y.-F. Huang, J.-J. Geng and Z.-B. Zhang, *Statistical study of gamma-ray bursts with a plateau phase in the x-ray afterglow*, *The Astrophysical Journal Supplement Series* **245** (2019) 1.

[23] A. de Ugarte Postigo, C.C. Thoene, J.F. Agui Fernandez, D.B. Malesani, Rakotondrainibe, N.R. Tanvir et al., *GRB 240529A: Redshift from GTC/OSIRIS+*, *GRB Coordinates Network* **36574** (2024) 1.

[24] D. Svinkin, D. Frederiks, M. Ulanov, A. Tsvetkova, A. Lysenko, A. Ridnaia et al., *Konus-Wind detection of GRB 240529A*, *GRB Coordinates Network* **36584** (2024) 1.

[25] W. Atwood, A. Albert, L. Baldini, M. Tinivella, J. Bregeon, M. Pesce-Rollins et al., *Pass 8: Toward the full realization of the fermi-lat scientific potential*, 2013.

[26] P. Bruel, T.H. Burnett, S.W. Digel, G. Johannesson, N. Omodei and M. Wood, *Fermi-lat improved pass 8 event selection*, 2018.

[27] J. Ballet, T.H. Burnett, S.W. Digel and B. Lott, *Fermi large area telescope fourth source catalog data release 2*, 2020.

[28] T. Fukushima, S. To, K. Asano and Y. Fujita, *Temporal Evolution of the Gamma-ray Burst Afterglow Spectrum for an Observer: GeV-TeV Synchrotron Self-Compton Light Curve*, **844** (2017) 92 [1706.07537].

[29] K. Asano, K. Murase and K. Toma, *Probing Particle Acceleration through Broadband Early Afterglow Emission of MAGIC Gamma-Ray Burst GRB 190114C*, **905** (2020) 105 [2007.06307].

[30] C.T.A. Observatory and C.T.A. Consortium, *CTAO Instrument Response Functions - prod5 version v0.1*, Sept., 2021. 10.5281/zenodo.5499840.

[31] H. Abe, S. Abe, V.A. Acciari, I. Agudo, T. Aniello, S. Ansoldi et al., *Magic detection of grb 201216c at z = 1.1*, *Monthly Notices of the Royal Astronomical Society* **527** (2023) 5856 [https://academic.oup.com/mnras/article-pdf/527/3/5856/54082772/stad2958.pdf].